http://dx.doi.org/10.5012/bkcs.2013.34.9.2781

AC Complex Impedance Study on the Resistive Humidity Sensors with Ammonium Salt-Containing Polyelectrolyte using a Different Electrode Pattern

Jae-Ryung Cha and Myoung-Seon Gong*

*Department of Nanobiomedical Science and WCU Research Center of Nanobiomedical Science, Dankook University, Cheonan, Chungnam 330-714, Korea. *E-mail: mgong@dankook.ac.kr*
Received April 8, 2013, Accepted June 17, 2013

We examined the effect of electrode fingers and gaps of coplanar interdigitated electrode (IDE) structures to characterize the ammonium salt-containing polyelectrolyte film of resistance-based humidity sensors. IDEs designed for this purpose were flexible gold electrodes deposited on a polyimide substrate using a printing process because the geometry presents a potential for tunable sensitivity over other electrode designs. The basic design of the sensors consisted of IDEs with a different number of electrode fingers such as 3, 4, and 5 and gap sizes of 310, 360, 410, and 460 μm. Details of the AC complex impedance characteristics such as the Nyquist plot, Bode plot, and activation energy based on electrode construction were investigated.

Key Words : Resistive humidity sensor, Bode plot, Nyquist plot, Interdigitated electrode, Electrode pattern

Introduction

Humidity sensors have attracted increasing attention because of the growing demand for accurate measurement and control of environment humidity in many fields.[1-5] In recent years, more attention has been paid to resistive-type polymeric humidity sensors, where hydrophilic vinylpolymers bearing quaternary ammonium salt are used as the humidity-sensing materials, because of advantages of high humidity sensitivity, fast response, low cost, easy preparation, etc.[6-17]

Several electrode geometries have been developed during the last few decades to lower the detection limit of humidity sensors. A combination of physical and numerical modeling has been used to investigate the use of coplanar interdigitated electrode (IDE) structures with different electrode geometries to measure the electrical resistance of sensing materials.[18,19] It is often necessary to control electrode length by concentrating a simple two-electrode strip-line into an IDE structure to achieve measurable resistances.[20-23]

If the number of fingers and the gap size sufficiently affect the humidity-sensitive characteristics of the sensors, the impedance between a pair of electrode fingers can be controlled or tuned by the electrode configurations.[18,19,24,25] Sensor characteristics including sensitivity, linearity, temperature dependence, and response time on electrode construction were examined using flexible humidity sensors with a gold electrode/glass epoxy substrate. However, the main drawback was the small variations in their intrinsic resistances; the variations were so small that no significant difference was detected between the samples.[26,27] Therefore, it is necessary to measure other electrical properties of the sensor to maximize sensitivity so that the AC complex impedance characteristics can be investigated when assessing a humidity sensor with different electrode configurations.[26-29]

In general, characteristics of the humidity sensor were related with the chemical structures of the humidity-sensitive polyelectrolyte[1-3,6-8] including their ionic moieties, such as cationic, anionic, and amphoteric, and their counter ions.[4,5,9-14] The thickness of the polyelectrolyte closely affects the humidity sensitivities, such as hysteresis and response or recovery time.[15,16] In addition, IDEs-type humidity sensors exhibited a significant change in impedance with a change in the number of fingers and gap size between electrode fingers, which are related to the design of the electrode. For practical applications, these techniques are expected to optimize the humidity-sensing characteristics precisely.[26-29]

In this study, 11 IDEs with a different number of electrode fingers such as 3, 4, and 5 and gap sizes of 310, 360, 410, and 460 mm were prepared using screen printing technology. AC complex impedance characteristics such as Nyquist plots and Bode plots including activation energy for the resistive humidity sensors with quaternary ammonium salt-containing polyelectrolyte using various electrode structures were evaluated.

Experimental

Materials and Equipments. [2-(Methacryloyloxy)ethyl] propyl dimethyl ammonium bromide (MEPAB) was synthesized by a quaternization reaction of 2-(*N,N*-dimethylamino)ethyl methacrylate with *n*-propyl bromide.[16] Methyl methacrylate (MMA), ethylene glycol (EG), and azobisisobutyronitrile (AIBN, Aldrich Chemical, St. Louis, MO, USA) were used as received. 2-Methoxyethanol was dried with calcium hydride and sodium metal and purified by distillation.

A humidity and temperature controller (Jeio Tech Seoul, South Korea, model: TM-NFM-L; 20-95% relative humidity) was used to measure relative humidity (RH) at a constant temperature. The impedance was measured with an impedance analyzer (HP 4194). A rotation viscometer (Physica

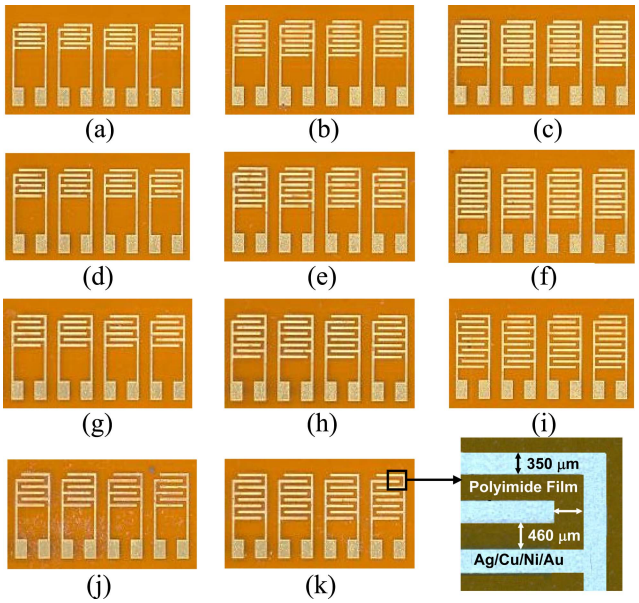

Figure 1. Photos of electrodes with various number of finger and gap size used in experiment; (a) 3 fingers, 310 mm of gap, (b) 4, 310, (c) 5, 310, (d) 3, 360, (e) 4, 360, (f) 5, 360, (g) 3, 410, (h) 4, 410, (i) 5, 410, (j) 3, 460, and (k) 4, 460.

UM) with a cone-plate measuring system was used to investigate viscosity dependant on shear rate. The electrodes were made by printing nano-silver paste (thickness 6-7 μm), followed by electroless plating of Cu (thickness 5 μm), Ni (thickness 2 μm), and then Au (thickness 80 nm), as previously reported.[30,31] Figure 1 shows photos of a set of 11 different humidity sensors with 3, 4, or 5 fingers and gap sizes of 310, 360, 410, and 460 mm between fingers on a PI substrate.

Preparation of Humidity-sensitive Printing Ink. A mixture of MEPAB (14.43 g, 50 mmol), METAC (4.15 g, 20 mmol), MMA (2.00 g, 25 mmol) and AIBN (0.09 g, 0.56 mmol) were dissolved in anhydrous EG/2-methoxyethanol (v/v = 70/30, 100 g) in a three necked round-bottomed flask (500 mL) equipped with an N_2 inlet system and a mechanical stirrer. The solution was degassed by bubbling N_2 gas for 30 min. The flask was heated to 65 °C for 24 h. After the polymerization was completed, Flow 425 (0.2 wt % of printing ink, Tego Co.) was added to the mixture as a leveling agent.

Fabrication of a Humidity-sensitive Membrane. A thin polymeric resistive humidity-sensitive film was formed on the electrode/PI using the screen printing method. After screen printing (polyester screen 68 T), wet decorations were dried for 30 min at 50 °C and 1 h at 130 °C in a preheated convection oven. The dried thickness and area of the film were 8-10 μm and 25-45 μm^2 for each sensor. The sensors were electrically tested after bonding of lead wires to the sensor chip terminal using a silver-loaded conductive adhesive.

Impedance Characteristic Measurements. Impedance *vs.* RH characteristics of the sensors were measured between 20-95% RH at 1 V and 25 °C. The measurement of humidity

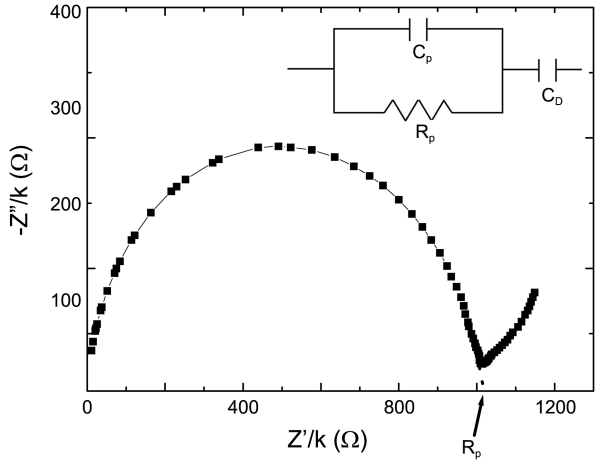

Figure 2. General Cole-Cole plot and its equivalent circuit (R_P, resistance; C_P, capacitance; C_D, double-layer capacitance).

detection output is done after 10 minutes have passed after the temperature and humidity setting. A simple equivalent circuit of a parallel combination of the resistance (R_P) and capacitance (C_P), plus the double-layer capacitance (C_D), at the interface between the polyelectrolyte and the electrodes for the impedance spectroscopy were assumed. The value of the parallel resistance, R_P, was estimated by extrapolating the semicircle or the pile to the real axis based on the assumption of an equivalent circuit.

Results and Discussion

Printable polyelectrolyte ink must be formulated to fit the physical and rheological requirements of fluid flow during the printing process. The polyelectrolyte ink was simultaneously prepared by radical copolymerization of MEPAB and MMA in EG/2-methoxyethanol (v/v = 7/3) with AIBN at 65 °C as shown in Scheme 1. MEPAB and MMA were used as a humidity-sensitive monomer and controller for the humidity-sensing characteristic, respectively. Viscosity, thixotropic index, and surface tension of the printing ink were the main parameters governing the fabrication conditions of humidity-sensitive films. The printable polyelectrolyte ink showed a viscosity of 2400 cps, and thixotropic rheology was obtainable from the appropriate ratio of EG to 2-methoxyethanol, so it could be printed from a silk-screen.[16,17,30] Polyelectrolyte films were printed on IDEs/PI substrate using a screen printer. After the ink was printed on the electrode, it was heated to produce humidity-sensitive film after evaporation of the solvents.

AC complex impedance spectroscopy (Nyquist plot) provided a powerful tool to analyze the electrical interaction of the humidity-sensitive material as well as to understand the effects of electrode structures on the electrical properties in detail.[31,32] Therefore, experiments with AC complex impedance spectroscopy were carried out in the frequency ranging from 40 Hz to 1 MHz. Figure 3(a) shows the Nyquist plots at various RH levels. These plots exhibit two types of impedance such as the semicircle-type and straight line-type

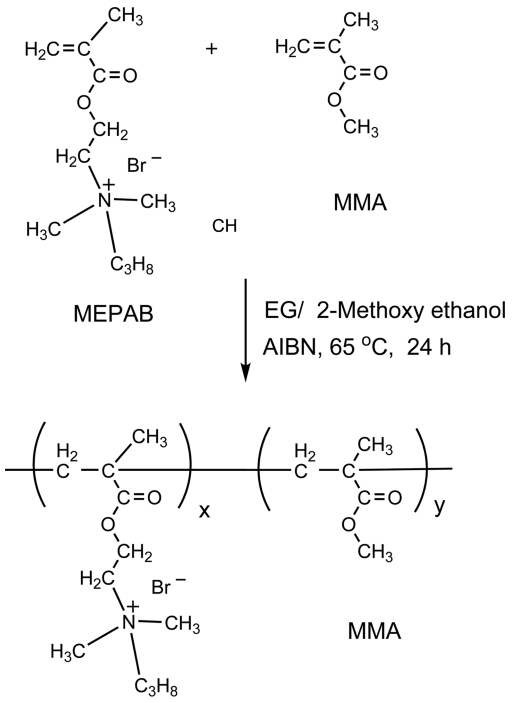

Scheme 1

impedances. At a sufficiently low RH, they were composed of semicircles prolonged with curved lines for the low frequency values, which could be modeled by an equivalent parallel resister and a capacitor circuit. With increasing humidity, a semicircle was connected with the straight line-type impedance, which was caused by diffusion of ions across the interface between the polyelectrolyte films and the electrodes.[31,32]

Figure 3(b) shows the Nyquist plot of the three different humidity sensors with 3, 4 and 5 fingers and a gap size of 360 μm at 60% RH. All curves exhibited similar variation tendencies. The impedance proportionally decreased with increasing number of fingers from 3 to 5. Here, we defined detection sensitivity as the ratio of the change in output impedance to the change in the number of fingers. The sensitivity of the sensor was −70 ± 5 $\Omega W/N_{finger}$, indicating that high sensitivity was obtained.

In 3 fingers sensors, for each negative-positive finger, one resistance are going to be available. If this fingers increase, the resistance will decrease also. The association of this resistance could be parallel. Due to this association, $1/R_{total} = 1/R_1 + 1/R_2$ (for instance in case of 3 fingers) and $1/R_{total} = 1/R_1 + 1/R_2 + 1/R_3 + 1/R_4$ (for 5 fingers). Both cases have the same sensing material, and distance (gap) between fingers, due to that all Ri are the same R. Then, R_{total} for 3 fingers is R/2, and for 5 fingers is R/4, less resistance. Moreover, this description could explain how different gaps affect to impedance and how the sensors with 3 fingers provide bigger relative changes with water than 5 fingered sensors.

The gap size between fingers also highly affected the sensing characteristics in the Nyquist plots as shown in Figure 3(c). As the gap size increased from 310 to 460 μm, impedance increased constantly. The influence of gap size between fingers on the impedance appeared to be similar for

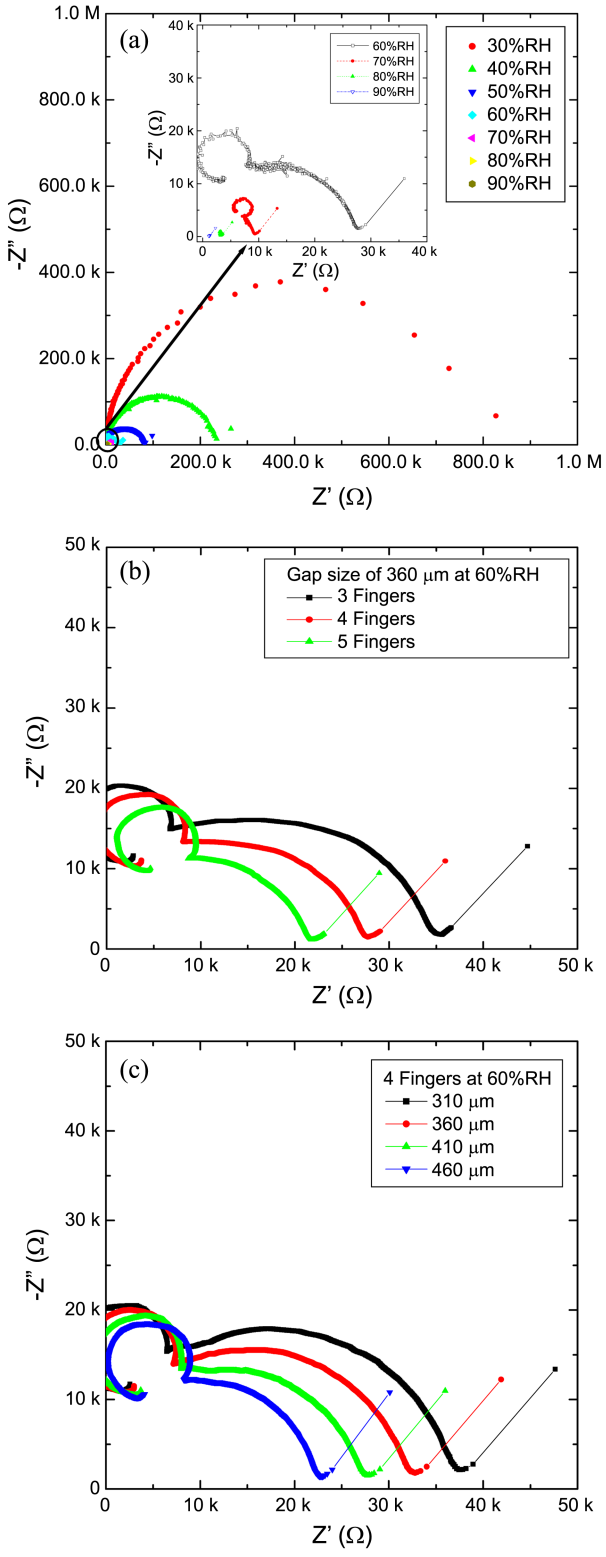

Figure 3. Nyquist plots for the sensor with (a) 4 fingers and a gap size of 360 μm at 30-90%RH, (b) 3, 4 and 5 fingers and a gap size of 360 μm, and (c) 4 fingers and a gap size of 310, 360, 410 and 460 μm at 60%RH.

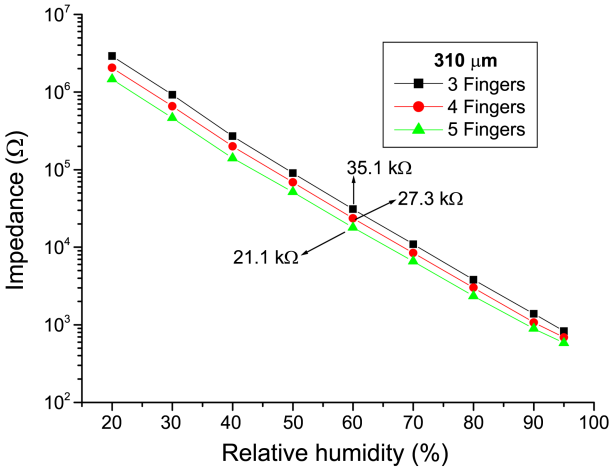

Figure 4. Impedance dependence on the humidity sensors with 3, 4 and 5 fingers and a gap size of 310 μm at 25 °C, 1 kHz and 1 V.

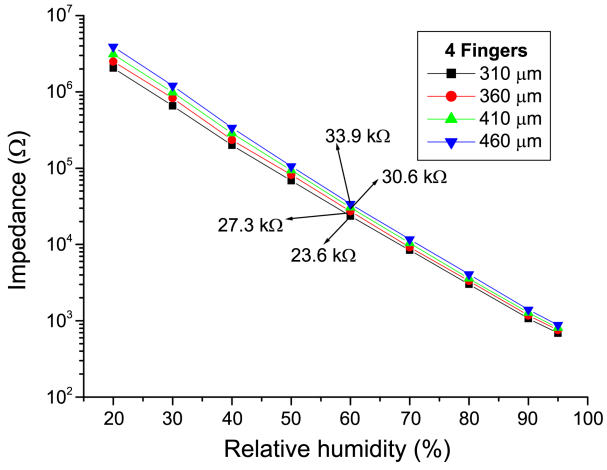

Figure 5. Impedance dependence on the relative humidity of the sensors with 4 fingers and various gap size at 25 °C, 1 kHz and 1 V.

sensors with different fingers; that is, an increase in gap size increased impedance. When impedance changes in sensors with 5 fingers and gap sizes of 310, 360, and 410 μm were compared with those with 3 or 4 fingers, similar patterned parallel curves were observed.

In the humidity range of 20-95% RH, the impedance variation of the humidity sensors with 3, 4, and 5 fingers and a gap size of 310 μm was 3.70 MΩ-1.56 kΩ, 3.08 MΩ-1.08 kΩ, and 2.51 MΩ-0.73 kΩ, respectively, as shown in Figure 4. The humidity sensor with 5 fingers displayed much lower impedance than that of 3 fingers. The impedance of the sensor with 5 fingers (21.1 kΩ) and a gap size of 360 μm was 39.9% smaller than that of 3 fingers (35.1 kΩ) at 60% RH. The increase in the number of fingers caused a decrease in impedance because of the increase in the number of migrating ions. Hence, total conduction was the sum of currents of individual electrode pairs. These tendencies correlated well with the theory for the capacitance of IDE structure with 3 or more fingers.[18,19]

The impedance of the sensor with 4 fingers and a gap size of 310 μm (23.6 kΩ) was 30.4% smaller than that of 4 fingers and a gap size of 460 μm (33.9 kΩ) at 60%RH as shown in Figure 5. The increase in the gaps between the fingers caused a decrease in impedance. The changes in the impedance of the sensors were similar at the low and high humidity range. The increase in gap size hindered the ions from migrating exceeding the potential barrier from one finger position to the others. These results suggest that the number of electrode fingers and gap size affected the sensing characteristics of the sensors using the same polyelectrolyte throughout the entire humidity range. Resistance R is given by $R= \rho xd/Lxl$ for a thin film coated on coplanar electrodes, where ρ is the resistivity of the thin film, l is its thickness, d is the gap size between the electrodes, and L is their length. Electrode width does not appear in the formula because the width of the electrodes is always much larger than the thickness of the sensing film. The results are in satisfactory agreement with the coplanar electrodes model suggested by Ménil.[18,19]

Bode plots are also a useful method to understand impedance changes at various frequency levels. When impedance is plotted against frequency, a constancy in impedance with frequency is observed for all the sensors in the humidity range of 20-95% RH. The values of log|Z|/Ω of the sensor proportionally decreased with increasing RH. In particular, an abrupt decrease in impedance was exhibited at the low humidity range as shown in Figure 6(a). The average humidity coefficient between 30 and 90% RH was −0.05 ± 0.005 log|Z|/Ω·%RH for the sensors in the range of 10 Hz-100 kHz.

Figure 6(b) shows the Bode plots in the 0.1 Hz-0.5 MHz range at 25 °C for the electrodes with 3, 4, and 5 fingers and a gap of 360 μm at 60%RH. A monotonous decrease in impedance was observed for the sensor in the low frequency region up to 0.5 MHz, followed by an abrupt decrease at high frequencies > 0.5 MHz. The impedance proportionally decreased with an increase in the number of fingers from 3 to 5. The sensitivity of the sensor was −0.25 ± 0.02 $\log|Z|/\Omega \cdot N_{finger}$. Figure 6(c) shows the Bode plots for the sensors with different gap sizes and 3 fingers at 60% RH. Impedance decreased gradually with an increase in frequency up to 500 kHz at 60% RH. The impedance increased with an increase in gap size. The results obtained from the Nyquist plot are coincident with those of the Bode plot.

Changes in activation energy were calculated to understand the ion conduction of the various sensors with different electrode patterns according to the equation $R_P = R_o\exp(E_a/kT)$ between 30-90%RH. The resistance (R_p) of the sensor followed the Arrhenius equation, with straight line plots for the semi-log of the resistance against 1/T. In the case of the sensor with 5 fingers and a gap size of 410 μm, the variation in activation energy changed from 0.369 eV to 0.122 eV between 30 and 90% RH as shown in Figure 7. Slightly lower activation energy was observed for sensors with a greater number of fingers and a narrower gap size as shown in Table 1. The activation energy decreased from 0.152 to 0.122 eV with an increase in the number of fingers from 3 to 5 at 90% RH. Activation energy is a function of the number

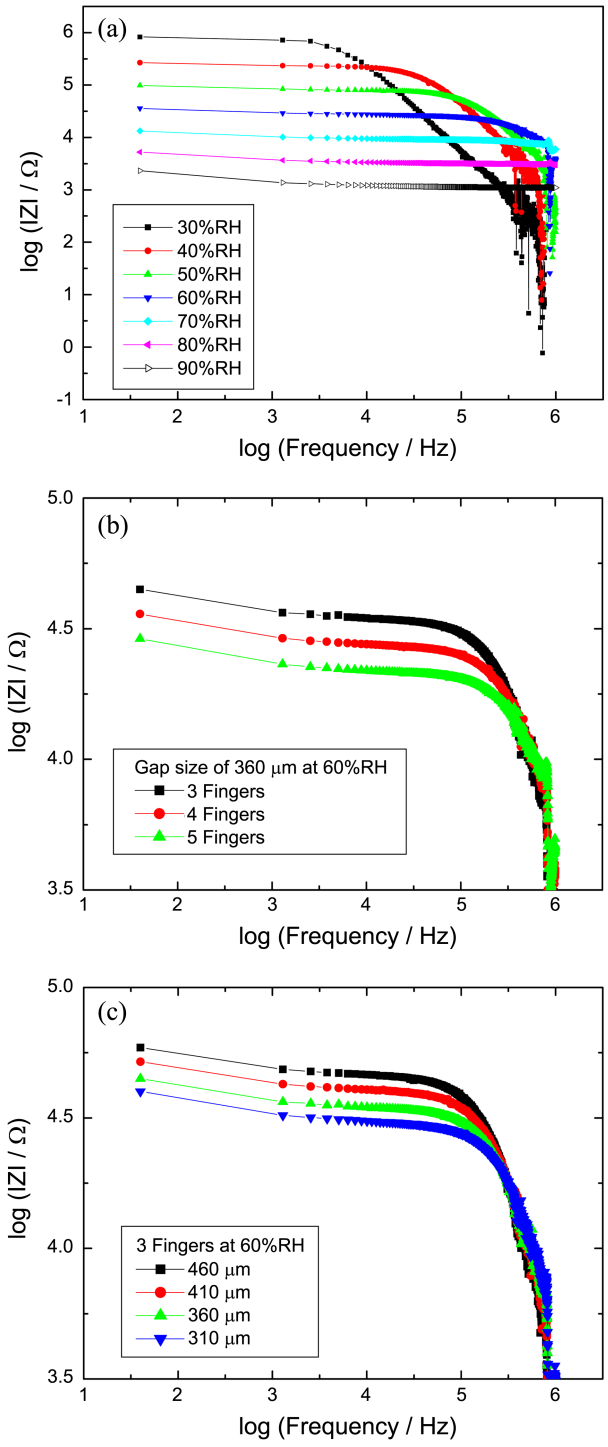

Figure 6. Bode plots for the sensor with (a) 4 fingers and a gap size of 410 μm at 30-90%RH, (b) 3, 4 and 5 fingers and a gap size of 360 μm, and (c) 4 fingers and a gap size of 310, 360, 410 and 460 μm at 60%RH.

of electrode fingers and the gap size between them.

Conclusion

Polymeric resistive humidity sensors were prepared by printing polyelectrolyte film onto electrode/polyimide with a different number of fingers and gap size. Impedance of the sensors responded proportionally to changes in RH over a range of 20-95%. These sensors exhibited a significant change in impedance with an increase in the number of fingers and gap size between them. Subsequent sensors will exhibit further control of humidity-sensing characteristics by changing the intrinsic properties of the polyelectrolyte as well as the electrode pattern. These results provide a simplified IDE model, which is a rough but straightforward estimate of the impedances of sensors with different IDE patterns.

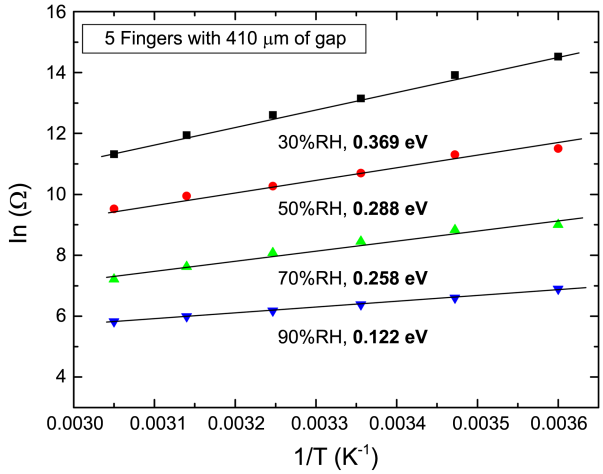

Figure 7. Arrhenius plot of resistance for the humidity sensor with 5 fingers and a gap of 410 μm.

Table 1. The activation energy for the sensors with different gap size and number of fingers

RH (%)	Fingers (ea)					
	3		4			5
	Gap (μm)					
	410	310	360	410	460	410
	Activation Energy (eV)					
30	0.407	0.348	0.362	0.384	0.478	0.369
50	0.336	0.263	0.281	0.307	0.362	0.288
70	0.299	0.226	0.2.52	0.276	0.296	0.258
90	0.152	0.111	0.123	0.139	0.152	0.122

Acknowledgments. The present research was conducted by the research fund of Dankook University in 2011.

References

1. Sakai,Y.; Sadaoka, Y.; Matsuguchi, M. *Sens. Actuators B* **1996**, *35*, 85.
2. Jeon,Y. M.; Gong, M. S. *Macromol. Res.* **2009**, *17*, 227.
3. Koo, J. S.; Gong, M. S. *Macromol. Res.* **2012**, *20*, 1226.
4. Sakai, Y.; Matsuguchi, M.; Yonesato, N. *Electrochim. Acta* **2001**, *46*, 1509.
5. Liu, K.; Li, Y.; Hong, L.; Yang, M. *Sens Actuators B* **2008**, *129*, 24.
6. Su, P. G.; Wang, C. P. *Sens. Actuators B* **2008**, *129*, 538.
7. Li, Y.; Chen, Y.; Zhang, C.; Xue, T.; Yang, M. *Sens. Actuators B* **2007**, *125*, 131.
8. Han, D. S.; Gong, M. S. *Macromol. Res.* **2010**, *18*, 260.

9. Su, P. G.; Uen, C. L. *Sens. Actuators B* **2005**, *107*, 317.
10. Han, D. S.; Gong, M. S. *Sens. Actuators B* **2010**, *147*, 330.
11. Gong, M. S. *Sens Actuators B* **2010**, *148*, 559.
12. Han, D. S.; Gong, M. S. *Macromol. Res.* **2011**, *19*, 679.
13. Han, D. S.; Gong, M. S. *Sens. Actuators B* **2010**, *145*, 254.
14. Sakai, Y.; Matsuguchi, M.; Hurukawa, T. *Sens. Actuators B* **2000**, *66*, 135.
15. Lee, I. H.; Gong, M. S.; Park, C. K. *Polymer (Korea)* **2009**, *33*, 326.
16. Kim, M. J.; Gong, M. S. *Analyst* **2012**, *137*, 1487.
17. Cha, J. R.; Gong, M. S. *Sens. Actuators B* **2013**, *178*, 656.
18. Kinder, N. J.; Homrighaus, Z. J.; Mason, T. O.; Garboczi, E. J. *Thin Solid Films* **2006**, *496*, 539.
19. Ménil, F.; Coillard, V.; Debéda, H.; Lucat, C. *Sens. Actuators B* **2001**, *77*, 84.
20. Al-Shareef, H. N.; Dimos, D.; Raymond, M. V.; Schwartz, R. W.; Mueller, C. H. *J. Electroceram*. **1997**, *2/1*, 145.
21. Hoerman, B. H.; Ford, G. M.; Kaufmann, L. D.; Wessels, B. W. *Appl. Phys. Lett*. **1998**, *73*, 2248.
22. Song, Z. T.; Chan, H. L. W.; Choy, C. L.; Lin, C. L. *Microelectron. Eng*. **2003**, *66*, 887.
23. Pond, J. M.; Kirchoefer, S. W.; Chang, W.; Horwitz, J. S.; Chirsey, D. B. Microwave *Integr. Ferroelectr.* **1998**, *22*, 317.
24. Lee, Y.; Yang, M. J.; Camaioni, N.; Casalbore-Miceli, G. *Sens. Actuators B* **2001**, *77*, 625.
25. Stephen, A. W.; Renaud, P. J. J.; Qi, Z. *et al. Mater. Sci. Eng. R* **2007**, *56*, 1.
26. Ahn, H. Y.; Kim, J. G.; Gong, M. S. *Macromol. Res*. **2012**, *20*, 174.
27. Ahn, H. Y.; Gong, M. S. *Polymer (Korea)* **2012**, *36*, 169.
28. Fürjes, P.; Kovács, A.; Dücsö, Cs.; Ádáma, M.; Müller, B.; Mescheder, U. *Sens. Actuators B* **2003**, *95*, 140.
29. Rittersma, Z. M. *Sens. Actuators B* **2002**, *96*, 196.
30. Cha, J. R.; Gong**,** M. S. *Sens. Actuators B* **2011**, *160*, 1082.
31. Su, P. G.; Huang, L. N. *Sens. Actuators B* **2007**, *123*, 501.
32. Shriver, D. S.; Bruce, P. G. Polymer electrolytes. I. General Principles, In: Bruce, P. G., Ed.; *Solid State Electrochemistry*; Cambridge University Press: Cambridge, 1995; p 95.